



Modelling of interfacial transition zone effect on resistance to crack propagation in fine-grained cement-based composites

H. Šimonová, M. Vyhídal, B. Kucharczyková, P. Bayer, Z. Keršner

Brno University of Technology, Faculty of Civil Engineering, Veveří 331/95, 602 00 Brno, Czech Republic

simonova.h@vutbr.cz, <http://orcid.org/0000-0003-1537-6388>

Michal.Vyhidal@vutbr.cz

Barbara.Kucharczykova@vutbr.cz, <http://orcid.org/0000-0002-7123-5099>

bayer.p@fce.vutbr.cz

kersner.z@fce.vutbr.cz, <http://orcid.org/0000-0003-4724-6166>

L. Malíková, J. Klusák

Institute of Physics of Materials, Academy of Sciences of the Czech Republic, v. v. i., Žižkovova 22, 602 00 Brno, Czech Republic

malikova.l@fpm.vutbr.cz, <http://orcid.org/0000-0001-5868-5717>

klusak@fpm.cz

ABSTRACT. In this paper, the attention is paid to investigation of the importance of the interfacial transition zone (ITZ) in selected fine-grained cement-based composites for the global fracture behaviour. This is a region of cement paste around the aggregate particles which specific features could have significant impact on the final behaviour of cement composites with a crack tip nearby this interface under applied tension. The aim of this work is to show the basic interface microstructure by scanning electron microscopy (SEM) done by MIRA3 TESCAN and to analyse the behaviour of such composite by numerical modelling. Numerical studies assume two different ITZ thicknesses taken from SEM analysis. A simplified cracked geometry (consisting of three phases – matrix, ITZ, and aggregate) is modelled by means of the finite element method with a crack terminating at the matrix–ITZ interface. ITZ's modulus of elasticity is taken from *generalized self-consistent scheme*. A few conclusions are discussed based on comparison of the average values of the opening stress ahead of the crack tip with their critical values. The analyses dealing with the effect of ITZ's properties on the stress distribution should contribute to better description of toughening mechanisms in silicate-based composites.

KEYWORDS. Fine-grained concrete; Interfacial transition zone; Scanning electron microscopy; Three-point bending fracture test; Effective fracture toughness.



Citation: Šimonová, H., Vyhídal, M., Kucharczyková, B., Bayer, P., Keršner, Z., Malíková, L., Klusák, J., Modelling of interfacial transition zone effect on resistance to crack propagation in fine-grained cement-based composites, *Frattura ed Integrità Strutturale*, 41 (2017) 211-219.

Received: 28.02.2017

Accepted: 15.04.2017

Published: 01.07.2017

Copyright: © 2017 This is an open access article under the terms of the CC-BY 4.0, which permits unrestricted use, distribution, and reproduction in any medium, provided the original author and source are credited.



INTRODUCTION

Cement-based composites belong to traditional and broadly used building materials [1]. Despite their long-term using, the investigation of damage of elements made of such materials under static loading is still developing. Concrete, as representative of such composites, shows nonlinear, more precisely, quasi-brittle behaviour – the ability to carry load continues even after the deviation from the linear branch of load–displacement diagram until the peak point and then the decrease of loading force follows until the failure, so called tensile softening. On the other hand, the individual components of primarily considered two-stage composite, cement paste and aggregate, show very often brittle elastic behaviour. This difference in cement-based composites behaviour is caused by development of multiple microcracking predominantly in the so called interfacial transition zone (ITZ) [2] and others toughening mechanisms. The aim of this paper is quantification of basic mechanical fracture parameters of selected fine-grained cement-based composites – static modulus of elasticity, fracture toughness and fracture energy and investigation of effect of ITZ between cement matrix (MTX) and aggregate (AGG) on stress distribution in cement based composite with crack terminating at the ITZ–MTX interface.

INTERFACIAL TRANSITION ZONE (ITZ)

The existence of interfacial transition zone (originally „aureole de transition“) between aggregate and cement paste was introduced in the fifties of last century by Farran [3]. Properties of ITZ and its impact on behaviour of cement-based composites have been studied numerically and experimentally from many points of view since that. Number of publications concerned with mechanical properties of individual components of cement-based composites are connected with homogenization techniques, such as e. g. Mori-Tanaka scheme [4] or generalized self-consistent scheme [5] used in this paper to estimation of ITZ's elasticity modulus.

Although investigation of concrete fracture is connected with the recognition that for description of its structural behaviour are necessary other independent material parameters, such as fracture toughness [6, 7] and not only compressive/tensile strength, only a few publications about ITZ are concerned with this fact, e.g. [8, 9]. Fracture mechanics based on analytical-numerical approaches, mainly connected with finite element method (FEM), is widely used to simulate structural response of materials with internal defects (microcracks, voids, pores) which lead to initiation, propagation of cracks and consequent fracture. The problem with crack-interface interaction of two elastic materials is long-term investigated by team gradually created by prof. Kněsl from Institute of Physics of Materials of the Academy of Sciences of the Czech Republic, v. v. i. [10, 11].

EXPERIMENTAL PART

Materials and specimens

Two fine-grained cement-based composites mixtures with various water to cement (w/c) ratios and amount of plasticizer have been prepared for purpose of this study. Mixtures have been prepared on the basis of the standard CSN EN 1961 [12]. Portland cement type 42.5 R as a binder and quartz sand with the maximum nominal grain size of 2 mm standardize according to ČSN EN 196-1 [12] for the fine aggregate were used. The w/c ratio was different for both mixtures. The second mixture's w/c ratio was reduced by addition of super-plasticizer SVC 4035 in amount of 1 % by cement mass. Mixtures were prepared by a mixing device with controllable mixing speed. The basic information about the composition and properties of the fresh composites are given in Tab. 1. The properties of the fresh composites were determined in accordance with ČSN EN 1015-3 [13] and ČSN EN 1015-6 [14].

The three specimens of 1000 mm in length and with 60×100 mm in cross-section were made from each mixture and primarily used for recording the length changes. After the stabilization of shrinkage values, approximately after 90 days, the beam specimens with nominal dimensions $40 \times 40 \times 160$ mm were cut from these specimens and subsequently used for three-point bending fracture tests. This procedure was chosen primarily because of exclusion of specimen boundary effect. The specimens for microscopy measurements were prepared from former mentioned specimens.

Components and properties	Units	Composite ID	
		04042016	09052016
Quartz sand	[kg]	45.9	45.9
Cement I 42.5 R	[kg]	15.3	15.3
Super-plasticizer SVC 4035	% by cement mass	—	1.0
Water to cement ratio	[—]	0.5	0.35
Workability	[mm]	140	135
Bulk density	[kg/m ³]	2200	2280

Table 1: Composition and properties of fresh composites.

Fracture tests

The fracture tests in three-point bending were carried out using a Heckert FP 10/1 testing machine with measuring range of 0–2000 N. The beam specimens were provided by initial central edge notch with approximately depth 1/3 of specimen depth situated in the middle of span length; span length was 120 mm.

The displacement increment loading was performed, which allowed to record load versus displacement diagrams ($L-\delta$ diagrams) during the tests. The $L-\delta$ diagrams were used for the determination of elasticity modulus from the first (almost linear) part of the diagram, and for the calculation of effective fracture toughness using the effective crack extension method [15] and specific fracture energy using work-of-fracture method [16]. Because of stability loss during loading, it was not possible to reconstruct the descending part of $L-\delta$ diagrams. Therefore, the work of fracture W_F^* value is determined as area under $L-\delta$ diagrams before stability loss occurred. For details about determination above mentioned mechanical fracture parameters see [17].

The results of performed fracture tests evaluation are introduced in Tab. 2 in form mean values and standard deviations ordinarily from six specimens. The monitored mechanical fracture parameters were following: modulus of elasticity E , effective fracture toughness K_{Icc} and specific fracture energy G_F^* (determined using mentioned work of fracture W_F^* value).

Parameter	Units	Composite ID	
		04042016	09052016
Modulus of elasticity E	[GPa]	32.1 ± 1.6	34.2 ± 2.6
Fracture toughness K_{Icc}	[MPa·m ^{1/2}]	0.759 ± 0.054	1.093 ± 0.067
Fracture energy G_F^*	[J·m ⁻²]	10.76 ± 1.78	24.37 ± 2.89

Table 2: Selected fracture tests results of 04042016 and 09052016 composites.

Microstructure of tested specimen's material

Microscopy measurements for quantitative description of microstructure of ITZ were carried out using scanning electron microscopy (SEM) MIRA3 TESCAN. The projection of specimen's surface was performed using secondary electrons (SE) or backscattered electrons (BSE). The selected micrographs caused by detection of SE with accelerating voltage of electrons 20 kV are introduced bellow.

Microstructure of fracture surfaces at the aggregate–cement paste interface for both tested specimens are introduced in Fig. 1. SEM image of fracture surface of the specimen with greater w/c ratio (on the left) shows less compact microstructure in compare with the other one. It is possible to identify the elemental minerals forming interface, namely ettringite, portlandite and C-S-H gel. On the contrary, there wasn't found any ettringite on the right SEM image. It can be caused by random selection of fracture surface part.

The other advantage of SEM is a possibility of length measurements. It has to be mentioned that measurements are made on a two dimensional sections through a three dimensional microstructure. Nevertheless, the distances, used here for the primary information about size and shape of the ITZ, are uncorrected distances measured on 2D sections.



The measured values of distances between individual grains of aggregate are shown in Fig. 2. These distances, even though they don't correspond to the idealized concept of a thickness and shape of the ITZ, come from real measurements. These measurements prove that the formation of the discrete zone (ITZ) with constant thickness around grain of aggregate is practically impossible. Therefore, the distances between these individual grains and the larger one, or more precisely their mean values, are considered as the thicknesses of the ITZ in following study [2, 18].

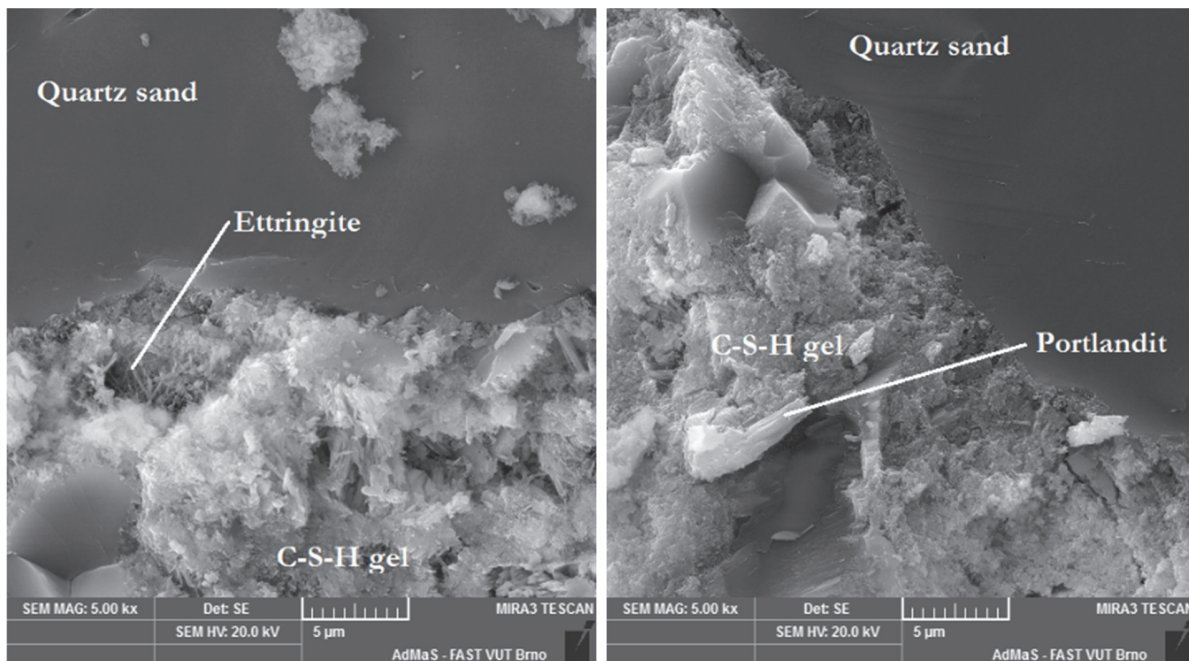


Figure 1: Microstructure of fracture surface at aggregate–cement paste interface by detection of SE with magnification 5000 \times , specimens 04042016 (left) and 09052016.

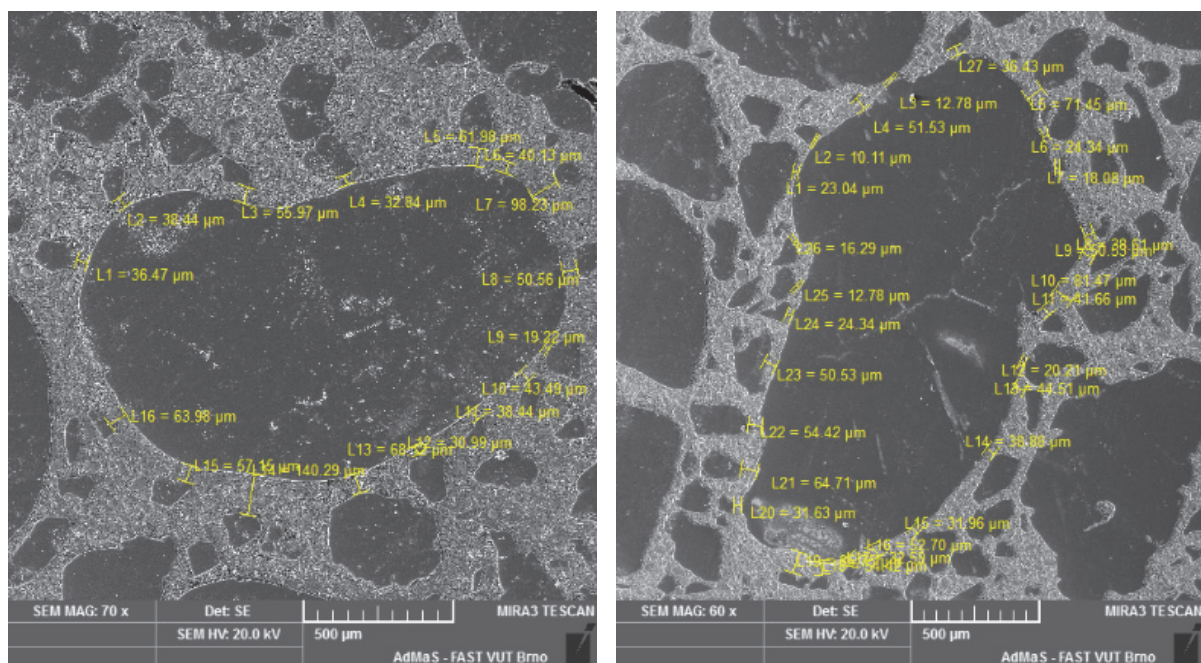


Figure 2: Distances between grains of aggregate measured using SEM with detection of SE, specimens 04042016 (left, magnification 70 \times) and 09052016 (magnification 60 \times).

NUMERICAL MODEL

A simplified model of the cracked specimen was created in ANSYS software to determine clearly the impact of the ITZ. Note that the configuration assumed is based on the three-point bending fracture test of a beam with central edge notch, see Fig. 3 (left). In the process of model creating the effects of the vertical position of inclusion, size of the aggregate and its circular shape were ignored. The crack was modelled by introduction of appropriate boundary conditions with its tip at the interface between MTX and ITZ, see the scheme in Fig. 3. Materials were modelled as linear, elastic and isotropic, which are represented by their elastic constants, i.e. Poisson's ratio ν and Young's modulus E . Thickness of ITZ for both composites was considered as the mean value of distance of individual grains of aggregate obtained from SEM micrographs, see Fig. 2. Modulus of elasticity value of cement paste (E_{MTX}) was taken from above mentioned results of fracture tests (see Tab. 2) and was statistically processed – the value of 5 % quantile ($E_{\text{MTX}, 0.05}$), mean value ($E_{\text{MTX}, \text{mean}}$) and 95 % quantile ($E_{\text{MTX}, 0.95}$) were taken into consideration. This simplification was chosen because of absence of nanoindentation tests and because of the same ratio of components (aggregate:cement) in both composites. The last information means that the elasticity modulus value of E_{MTX} is approximately k -multiple of elasticity modulus of the composite mentioned in Tab. 2. The elasticity modulus values of ITZ (E_{ITZ}) were considered as 50 % values of E_{MTX} according to the procedure called *generalized self-consistent scheme* [5]. The elasticity modulus value of aggregate (quartz sand) was taken from [19] as the mean value. The complex overview is introduced in Tab. 3.

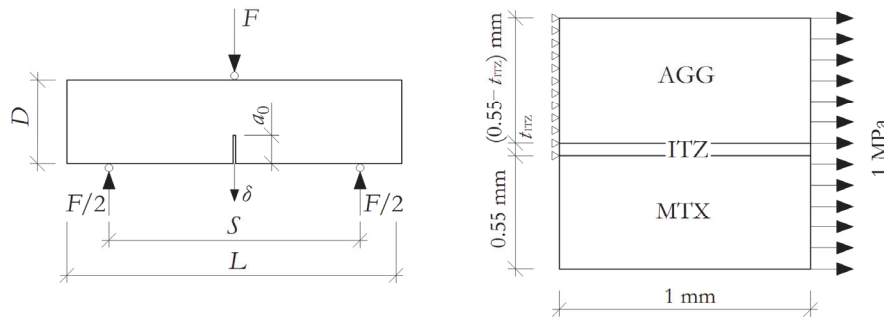


Figure 3: Scheme of the three-point bending fracture tests with central edge notch in the middle of span length (left), scheme of simplified 2D model of the cracked specimen created in software ANSYS.

Parameter	Units	Composite ID	
		04042016	09052016
Thickness of ITZ	[μm]	55	40
E_{MTX}	[GPa]	32.1 ± 1.6	34.2 ± 2.6
ν_{MTX}	[–]	0.21 [20]	0.21 [20]
E_{ITZ}	[GPa]	$0.5E_{\text{MTX}}$ [5]	$0.5E_{\text{MTX}}$ [5]
ν_{ITZ}	[–]	0.21 [20]	0.21 [20]
E_{AGG}	[GPa]	73 ± 1.6 [19]	73 ± 1.6 [19]
ν_{AGG}	[–]	0.20 [20]	0.20 [20]

Table 3: Overview of the elastic constants used in the numerical model.

RESULTS

For quantitative description of the influence of ITZ on the stress state in the crack tip vicinity the opening stress σ_{yy} is observed and evaluated. The mean stress $\bar{\sigma}_{yy}$ and the stress range $\Delta\sigma_{yy}$ are calculated:



$$\bar{\sigma}_{yy} = \frac{1}{d} \int_0^d \sigma_{yy}(x, y=0) dx, \quad (1)$$

$$\Delta\sigma_{yy} = \sigma_{yy,\max}^{\text{AGG}} - \sigma_{yy,\min}^{\text{ITZ}}, \quad (2)$$

where d is a size of region, where the stress is averaged.

For each configuration critical applied stress is evaluated by means of critical value of mean opening stress $\bar{\sigma}_{yyc}$ [21]:

$$\bar{\sigma}_{yyc} = \frac{2K_{lc}(\text{ITZ})}{\sqrt{2\pi d}} \quad (3)$$

Then the critical applied stress is:

$$\sigma_{\text{appl},c} = \sigma_{\text{appl}} \frac{\bar{\sigma}_{yyc}}{\bar{\sigma}_{yy}} \quad (4)$$

and it determines the magnitude of applied stress under which the crack will propagate through ITZ. In the following calculations it was taken $K_{lc} = 0.5 \text{ MPa}\cdot\text{m}^{1/2}$. This value is estimated as equal to usual fracture toughness of matrix of the composite.

Composites 04042016 and 09052016

As it was mentioned above the thickness of ITZ was taken from SEM measurement and in the composite 04042016 it was 55 μm , while in the composite 09052016 it was 40 μm .

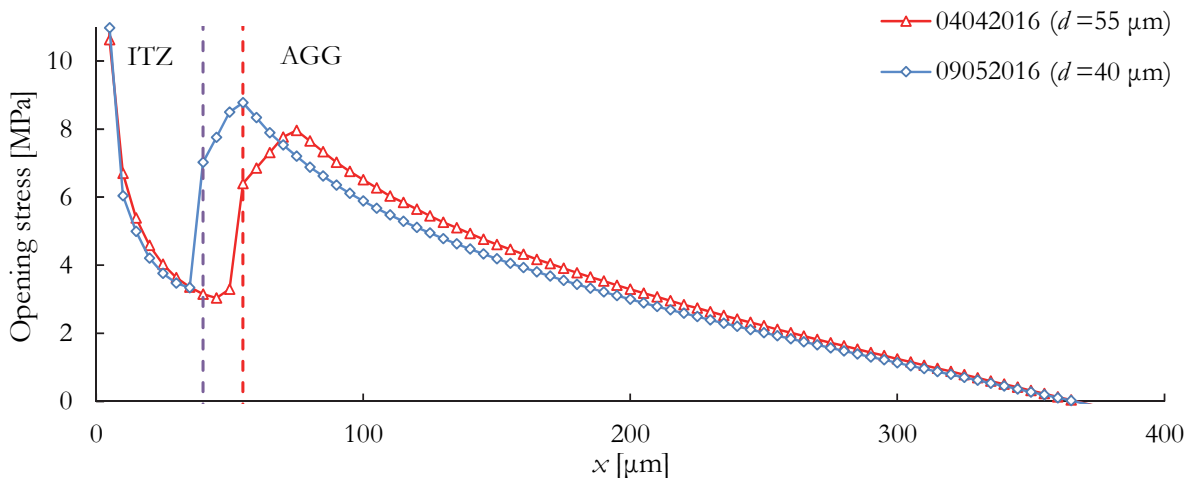


Figure 4: Distribution of the opening stress σ_{yy} in ITZ and AGG; ITZ thickness 55 μm and 40 μm .

In Fig. 4, the opening stresses σ_{yy} (for both composites) are shown in dependence on the distance from the crack tip x , where the value $x = 0 \mu\text{m}$ refers to the crack tip. The step changes of the stresses σ_{yy} are apparent at the interface between ITZ and AGG. Here the average values $\bar{\sigma}_{yy}$ are evaluated over the whole ITZ thicknesses. The average values $\bar{\sigma}_{yy}$ and the stress ranges $\Delta\sigma_{yy}$ for the composite 04042016 ($d = 55 \mu\text{m}$) are stated in Tab. 4 while for the composite 09052016 ($d = 40 \mu\text{m}$) they can be found in Tab. 5.

	E_{MTX} [GPa]	E_{ITZ} [GPa]	E_{AGG} [GPa]	$\bar{\sigma}_{yy}$ [MPa]	$\Delta\sigma_{yy}$ [MPa]	$\bar{\sigma}_{yyc}$ [MPa]	$\sigma_{\text{appl},c}$ [MPa]
$E_{\text{MTX},0.05}$	29.50	14.75	73.00 [19]	5.49	5.42	53.79	9.80
$E_{\text{MTX,mean}}$	32.10	16.05	73.00 [19]	5.90	4.92	53.79	9.12
$E_{\text{MTX},0.95}$	34.70	17.35	73.00 [19]	6.04	4.83	53.79	8.91

Table 4: The mean stress $\bar{\sigma}_{yy}$, its critical value $\bar{\sigma}_{yyc}$, stress range $\Delta\sigma_{yy}$ and critical applied stress $\sigma_{\text{appl},c}$ for various E_{MTX} and E_{ITZ} values considering the ITZ thickness 55 μm .

	E_{MTX} [GPa]	E_{ITZ} [GPa]	E_{AGG} [GPa]	$\bar{\sigma}_{yy}$ [MPa]	$\Delta\sigma_{yy}$ [MPa]	$\bar{\sigma}_{yyc}$ [MPa]	$\sigma_{\text{appl},c}$ [MPa]
$E_{\text{MTX},0.05}$	29.90	14.95	73.00 [19]	5.09	5.91	63.08	12.39
$E_{\text{MTX,mean}}$	34.20	17.10	73.00 [19]	5.54	5.43	63.08	11.39
$E_{\text{MTX},0.95}$	38.50	19.25	73.00 [19]	5.97	4.97	63.08	10.57

Table 5: The mean stress $\bar{\sigma}_{yy}$, its critical value $\bar{\sigma}_{yyc}$, stress range $\Delta\sigma_{yy}$ and critical applied stress $\sigma_{\text{appl},c}$ for various E_{MTX} and E_{ITZ} values considering the ITZ thickness 40 μm .

Comparison of results and their discussion

In the following, the main results obtained for both composites with different ITZ thickness values and elasticity moduli of MTX and ITZ are compared and discussed. The graphical expression of the dependences can be seen in Fig. 5 where the values of critical applied stress $\sigma_{\text{appl},c}$ are plotted in dependence on the elasticity modulus of ITZ.

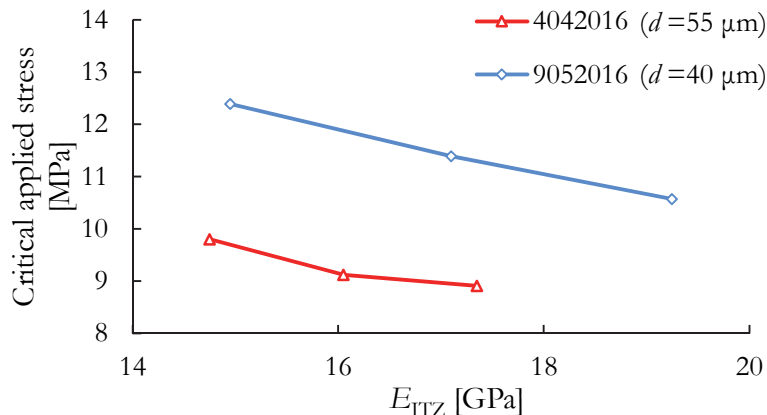


Figure 5: The values of the critical applied stress $\sigma_{\text{appl},c}$ in dependence on the elasticity modulus of ITZ.

The critical applied stress $\sigma_{\text{appl},c}$ corresponds to the level of the applied stress under which further crack propagation through ITZ is expected. The values of $\sigma_{\text{appl},c}$ are gained from the average values of the opening stress and their critical values. They depend on the distance d where the average stress is evaluated. We suppose that further crack propagation will occur by the crack increment through whole ITZ, we take d equal to the ITZ thickness and we can see that the results depend just on this. The plots in Fig. 5 clearly show that composites with thicker ITZ exhibit lower critical applied stress. Thus they violate easier than the composites with thinner ITZ. Similarly, it can be observed (from the Tabs. 4 and 5 and from the Fig. 5) that the stiffer ITZ leads (for particular ITZ thickness) to lower values of $\sigma_{\text{appl},c}$. These pilot results can lead to more reliable description of toughening mechanisms of composites of this kind. Further it can be used for design of more resistant silicate-based composites.



CONCLUSIONS

The authors focused their attention on the evaluation of the influence of the interfacial transition zone on the stress distribution in the cracked specimen. The crack tip was located at the interface between MTX and ITZ. As the average stress is used for stability criterion suggestion in cases of general singular stress concentrators [21], it can be used for quantification of the severity of the crack with its tip at a bi-material interface. Therefore, the opening stress σ_{yy} was observed and the average stress $\bar{\sigma}_{yy}$ ahead of the crack tip calculated. Not only the influence of the various ITZ thicknesses but also of various elastic moduli of ITZ on the near-crack-tip stress field was studied and discussed. Critical applied stress was evaluated based on knowledge of critical opening stress. Knowledge of the effect of the ITZ on the stress distribution will contribute to better understanding of the toughening mechanisms of the ITZ and aggregate in silicate-based composites.

ACKNOWLEDGEMENT

This outcome has been achieved with the financial support of the Czech Science Foundation under project No. 16-18702S “AMIRI – Aggregate-Matrix-Interface Related Issues in Silicate-based Composites”.

REFERENCES

- [1] Neville, A.M., Properties of Concrete, Pearson Education Limited, Harlow, (2011).
- [2] Scrivener, K.L., Crumbie, A.K., Laugesen, P. The Interfacial Transition Zone (ITZ) between Cement Paste and Aggregate in Concrete, *Interface Science*, 12 (2004) 411–421. ISSN 1573-2746. DOI: 10.1023/B:INTS.0000042339.92990.4c
- [3] Farran, J., Contribution mineralogique à l'étude de l'adhérence entre les constituants hydratés des ciments et les matériaux enrobés, *Revue des Matériaux de Construction*, 491 (1956) 155–157, 492 (1956) 191–209.
- [4] Mori, T., Tanaka, K., Average stress in matrix and average elastic energy of materials with misfitting inclusions, *Acta Metallurgica*, 21 (1973) 571–574. DOI: 10.1016/0001-6160(73)90064-3.
- [5] Hashin, Z., Monteiro, P.J.M., An inverse method to determine the elastic properties of the interphase between the aggregate and the cement paste, *Cement and Concrete Research*, 32 (2002) 1291–1300. DOI: 10.1016/S0008-8846(02)00792-5
- [6] Li, C.V., Maalej, M., Toughening in Cement Based Composites. Part I: Cement, Mortar and Concrete, *Cem Concr Comp.* 18 (1996) 223–237. DOI: 10.1016/0958-9465(95)00028-3
- [7] Shah, S.P., Fracture toughness of high strength concrete, *ACI Mater J*, 87 (1990) 260–265.
- [8] Wriggers, P., Moftah, S.O., Mesoscale models for concrete: homogenisation and damage behaviour, *Finite Elements in Analysis and Design*, 42 (2006) 623–636. DOI: 10.1016/j.finel.2005.11.008
- [9] Vervuurt, A., Van Mier, J.G.M., Fracture of the Bond Between Aggregate and Matrix: An Experimental and Numerical Study, In: A. Katz, A. Bentur, M. Alexander, G. Arlique, (eds.) RILEM Second International Conference on the Interfacial Transition Zone in Cementitious Composites, E & FN Spon, New York, (1998) 51–58.
- [10] Klusák, J., Profant, T., Kněsl, Z., Kotoul, M., The influence of discontinuity and orthotropy of fracture toughness on conditions of fracture initiation in singular stress concentrators, *Eng Fract Mech.* 110 (2013) 438–447. DOI: 10.1016/j.engfracmech.2013.05.002
- [11] Kněsl, Z., Klusák, J., Náhlík, L., Crack initiation criteria for singular stress concentrations, Part I–IV, *Eng Mech*, 14 (2007) 399–408, 409–422, 15 (2008) 99–114, 263–270.
- [12] ČSN EN 196-1:2005, Methods of testing cement – Part 1: Determination of strength, Prague: ČNI, 2005, (the Czech version of the European Standard EN 196-1:2005).
- [13] ČSN EN 1015-3:2000, Methods of test for mortar for masonry – Part 3: Determination of consistency of fresh mortar (by flow table), Prague: ČNI, 2000, (the Czech version of the European Standard EN 1015-3:2000).
- [14] ČSN EN 1015-6:1999, Methods of test for mortar for masonry – Part 6: Determination of bulk density of fresh mortar, Prague: ČNI, 1999, (the Czech version of the European Standard EN 1015-6:1999).



-
- [15] Karihaloo, B.L., Fracture mechanics and structural concrete, Wiley, New York, (1995).
 - [16] RILEM TC-50 FCM Recommendation, Determination of the fracture energy of mortar and concrete by means of three-point bend tests on notched beams, *Materials and Structures*, 18 (1985) 287–290.
DOI: 10.1007/BF02498757.
 - [17] Rovnaník, P., Šimonová, H., Topolář, L., Bayer, P., Schmid, P., Keršner, Z., Carbon nanotube reinforced alkali-activated slag mortars, *Construction and Building Materials*, 199 (2016) 223–229.
DOI: 10.1016/j.conbuildmat.2016.05.051
 - [18] Diamond, S., Huang, J., Interfacial Transition Zone: Reality or Myth? In: A. Katz, A. Bentur, M. Alexander, G. Arlique, (eds.) RILEM Second International Conference on the Interfacial Transition Zone in Cementitious Composites, E & FN Spon, New York, (1998) 3–39.
 - [19] Acker, P., Micromechanical analysis of creep and shrinkage mechanisms. In: F.J. Ulm, Z.P. Bažant, F., Wittman, (eds.) Creep, Shrinkage and Durability Mechanics of Concrete and other Quasi-Brittle Materials, Elsevier, Oxford, UK, (2001) 15–25.
 - [20] Sorelli, L., Constantinides, G., Ulm, F.J., Toutlemonde, F., The nano-mechanical signature of Ultra High Performance Concrete by statistical nanoindentation techniques, *Cement and Concrete Research*, 38 (2008) 1447–1456. DOI: 10.1016/j.cemconres.2008.09.002
 - [21] Knésl, Z., A criterion of V-notch stability, *Int J Fracture*, 48 (1991) R79–R83.